Rare Met. (2020) 39(8):902–908
https://doi.org/10.1007/s12598-017-0982-x

RARE METALS
www.editorialmanager.com/rmet

Processing and oxidation behavior of Pt-diffused coatings

Liang-Liang Wei, Hui Peng, Lei Zheng, Jing-Yong Sun, Hong-Bo Guo*

Received: 20 September 2016 / Revised: 26 October 2016 / Accepted: 1 November 2017 / Published online: 30 January 2018

Abstract Pt-diffused coatings were synthesized on Ni10Al alloy by electroplating a thin layer of Pt (1–5 μm) followed by a diffusion treatment in vacuum at 1000–1100 °C. Effects of processing parameters (Pt thickness and vacuum diffusion temperature) on the microstructures and chemical composition of Pt-diffused coatings were investigated. Also, the oxidation behavior of the coatings was studied at 1100 °C. Pt film reveals nano-sized grain size of 93–113 nm. Vacuum diffusion treatment leads to the grain growth. 1-μm Pt film with 1000 °C/1 h vacuum diffusion fabricates nano-sized Pt-diffused coating which exhibits the best oxidation resistance. And a single continuous Al_2O_3 scale forms on the coating with low Al (∼ 9 at%) and Pt (∼ 6 at%) contents. Increasing initial Pt thickness would introduce more defects and cracks, leading to a duplex scale and decreasing the oxidation resistance of Pt-diffused coatings.

Keywords Platinum-modified $\gamma + \gamma'$ coatings; Pt-diffused coatings; Electroplating; Oxidation; Nano-structure

L.-L. Wei, H. Peng, L. Zheng, H.-B. Guo*
School of Materials Science and Engineering, Beihang University, Beijing 100191, China
e-mail: guo.hongbo@buaa.edu.cn

H. Peng, H.-B. Guo
Key Laboratory of Aerospace Materials and Performance (Ministry of Education), Beihang University, Beijing 100191, China

J.-Y. Sun
School of Energy and Power Engineering, Beihang University, Beijing 100191, China

1 Introduction

Platinum-modified aluminide (Pt–Al) coatings have been used to provide oxidation resistance for Ni-based superalloy components of gas turbine engines for decades [1–6]. The content of Al in Pt–Al coatings should be higher than 40 at% to form a protective Al_2O_3 scale during high-temperature service. Unfortunately, high concentration of Al in coatings is not compatible with advanced Ni-base single-crystal (SC) superalloy which contains larger amount of refractory elements such as W, Ta, Re and Ru. Inward diffusion of Al from Pt–Al coatings to the underlying superalloy would lead to the formation of secondary reaction zone (SRZ) and needle-like topologically closed-pack phases (TCP), which are detrimental to the mechanical properties of the coated components [7–12].

Recently, a new type Pt–Al coating with low Al content, which is called Pt-diffused coatings (sometimes called Pt-modified $\gamma + \gamma'$ coatings or low-cost bond coats), has attracted increasing attention [13–18]. Pt-diffused coatings are usually produced by electroplating 5–10-μm Pt film on the superalloy, followed by a vacuum diffusion treatment. Without an aluminizing process, Al diffuses from the superalloy to the coatings by the uphill diffusion. It is believed that Pt-diffused coatings have several advantages over traditional Pt–Al coatings, including better compatibility with the Ni-based SC substrate (no TCP and SRZ precipitation during service), higher creep resistance (more resistant to mechanical damage), superior durability in thermal barrier coatings (TBC) system and low process cost (without aluminizing process).

Jiang and Gleeson [17] have suggested that the good oxidation resistance of Pt-diffused coatings results from high Pt contents, which can cause the Al uphill diffusion

from substrate. So most of the researchers have chosen high Pt thickness (more than 5 μm) and high vacuum diffusion temperature (1100–1190 °C) to maintain high Al and Pt concentration in coatings [19–21]. Similar to Pt–Al coatings, the oxidation performance of Pt-diffused coatings is also greatly affected by the substrate elements. For example, Hf is a beneficial element [22, 23], whereas S, Co and Ti are harmful elements for the oxidation resistance of the coating [24–28]. Outward diffusion of these harmful elements to the coating surface will cause degradation of oxidation resistance. However, high-temperature vacuum diffusion will accelerate the outward diffusion of these harmful elements; it is necessary to develop a low-temperature diffusion technique to produce Pt-diffused coatings which could minimize or diminish this negative effect.

Niu et al. [29] produced a 1.5-μm Pt film on a sputtered Ni_3Al coating, and an external Al_2O_3 scale was formed on the coating at 1050 °C in air. Here, 1.5-μm Pt is working to form an external Al_2O_3 scale without heat treatment. In the present work, Pt-diffused coatings were produced by thin Pt film (1–5 μm) and relatively low vacuum diffusion temperature (1000–1100 °C). The effects of processing parameters on high-temperature oxidation resistance of the coatings were investigated. In order to avoid the influence of substrate elements, Ni10Al alloy with 10 at% Al was used as the substrate materials.

2 Experimental

High-purity nickel and aluminum (purity higher than 99.99 at%) were used. The Ni10Al button was produced by arc melting, casted in argon atmosphere and then annealed in vacuum at 1150 °C for 24 h to ensure homogenization of the microstructure of the alloy. The chemical composition of annealed Ni10Al alloy is listed in Table 1. The concentration of sulfur impurity was also determined by inductively coupled plasma (ICP-AES, PHI700, Ulvacphi). Specimens were cut from the center of the button-shaped alloy into 10 mm × 8 mm × 3 mm, ground to 800-grit SiC finish and ultrasonically cleaned in alcohol and acetone prior to Pt plating.

Pt-diffused coatings were produced onto Ni10Al samples by electroplating Pt films with different thicknesses of 1, 3 and 5 μm, followed by 1-h vacuum heat treatment ($\sim 1.1 \times 10^{-4}$ Pa) at 1000 or 1100 °C. Cyclic oxidation tests of the coated samples were carried out in an air furnace equipped with an automation system which allows the specimens moving in and out of the furnace automatically. Each specimen was hung in a pre-annealed alumina crucible by Pt wire to collect all oxide spalls. A cycle includes 25-h heating in air furnace at 1100 °C and subsequent 10-min cooling out of the furnace to ambient temperature by compressed air. Mass changes were measured using an electronic balance (Sartorious CPA 225D, Germany) with a precision of 1×10^{-4} g. The mass changes for each coating were determined based on average weight changes of two specimens.

Table 1 Chemical composition of as-annealed Ni10Al alloy by ICP-AES

Elements	x_{Al}/at%	x_{Ni}/at%	$S/10^{-6}$
Concentration	10.02	Bal.	< 20

The surface and cross-sectional morphologies of the specimens were characterized by field emission scanning electron microscope (FE-SEM, Quanta 200F). The phases of Pt films and oxides were identified by X-ray diffractometer (XRD, Rigaku D/max2200 PC) using Cu Kα radiation. The chemical compositions of the coatings and oxides were determined by electron probe micro-analyzer (EPMA, JXA-8100). For cross-sectional observation, the specimens after 300-h oxidation were embedded in epoxy, ground and finely polished.

3 Results and discussion

3.1 Pt films by electroplating

After platinum electroplating, Pt films were characterized by XRD. The lattice constant of Ni crystal is 0.3524 nm (PDF 65-2865), while that of Pt is about 0.3923 nm (PDF 65-2868). At the beginning of plating, Pt atoms deposited as Ni lattice constant like epitaxial growth. When Pt thickness is up to 5 μm, the coating lattice changes to Pt lattice constant, as shown in Fig. 1. Curve 3 has almost the same peak position as standard Pt PDF card, while Curves 1 and 2 shift to right position, due to the influence of the substrate Ni10Al alloy. It can be inferred that the driving force of the mismatch between Ni10Al and 5-μm Pt film would introduce more defects than 1- and 3-μm Pt film specimens.

The grain size of Pt films was calculated from XRD data by Jade 5.0 software, as listed in Table 2. In order to calibrate the peak FWHM of XRD equipment, a standard Si powder XRD pattern was selected as reference. Pt films are composed of nano-sized grains.

3.2 Effect of Pt thickness

Vacuum diffusion treatment of three specimens with different Pt thicknesses was conducted at 1000 °C. For comparison, the specimen with 5-μm Pt film was also heat-

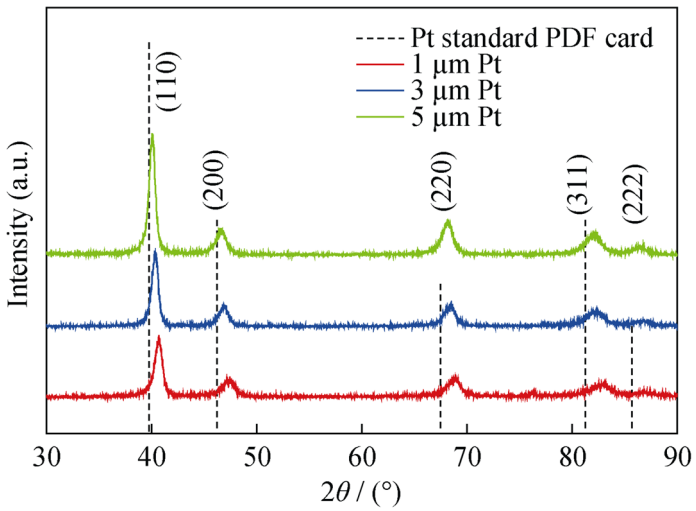

Fig. 1 XRD patterns of standard platinum card and 1-, 3- and 5-μm Pt films

Table 2 Average grain sizes of Pt films before and after 1000 °C diffusion calculated from XRD

Pt thickness/μm	Average grain size/nm	
	Before 1000 °C diffusion	After 1000 °C diffusion
1	93	267
3	110	341
5	113	405

treated in vacuum at 1100 °C. Hereinafter, the specimens with 1-, 3- and 5-μm Pt film diffused at 1000 °C are named as No. 1, No. 2 and No. 3, respectively, while the specimen with 5-μm Pt film diffused at 1100 °C is named as No. 4.

The coating surface elements concentrations were analyzed by EDS, as shown in Table 3. Al does not uphill diffuse from the substrate (10 at% Al) at 1000 °C. However, a little higher Al content is obtained when the diffusion temperature increases to 1100 °C. It has been shown by Gleeson et al. [30] that the concentration of Pt and Al affects the selective oxidation of Al in Ni–Pt–Al alloy at 1150 °C. In such low Al content (10 at%), a duplex-scale structure is formed on the alloy even the concentration of Pt is up to 25 at%. In this study, Al content is low (no more than 11 at%), Pt content is from 6 at% to 25 at%.

The oxidation of all specimens was performed in air at 1100 °C. The mass changes of Pt-diffused coatings on Ni10Al alloys are compared in Fig. 2. It should be noted that the coating with 1-μm Pt film diffused at 1000 °C reveals the lowest mass change among all four coatings. Surface and cross-sectional morphologies of the specimens after 300-h oxidation at 1100 °C are shown in Figs. 3 and 4. The corresponding surface chemical composition is given in Table 4. According to XRD result in Fig. 5, external Al_2O_3 scales are formed on No. 1, 2 and 4 specimens. Surface morphologies (Fig. 3a, b, d) are very similar with the oxide scale grown on β-NiAl coating, showing typical worm-like ridge structure.

The spallation of the oxide scale can be seen in No. 3 specimen (Fig. 3c). Combining XRD (Fig. 5) and surface chemical composition results, it can be determined that the bright area is $NiAl_2O_4$ with residual small Pt particles, while the dark area is Al_2O_3. As seen in Fig. 4c, the scale of No. 3 specimen consists of outer $NiAl_2O_4$ spinel layer and inner Al_2O_3 layer.

Table 3 Processing parameters and surface element concentrations of Pt-diffused coatings

No.	Pt thickness/μm	Temperature/°C	Time/h	Surface elements/at%		
				Pt	Al	Ni
1	1	1000	1	6.36	9.25	Bal.
2	3	1000	1	15.65	9.07	Bal.
3	5	1000	1	25.81	8.71	Bal.
4	5	1100	1	18.41	10.89	Bal.

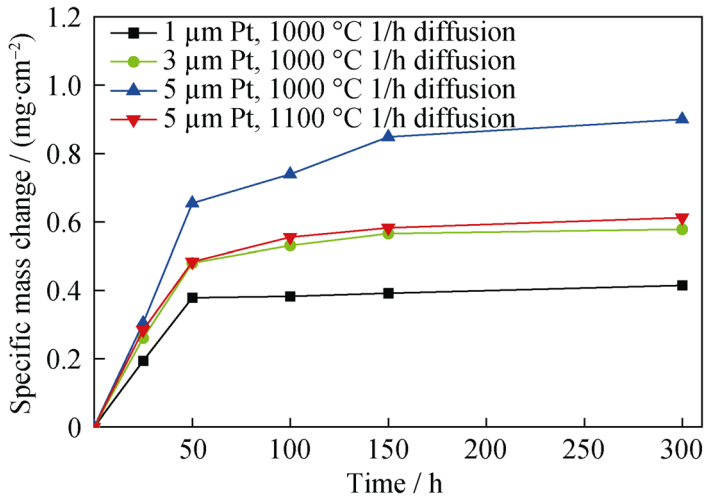

Fig. 2 Weight changes of Pt-diffused coatings on Ni10Al alloy at 1100 °C/300-h oxidation test in still air

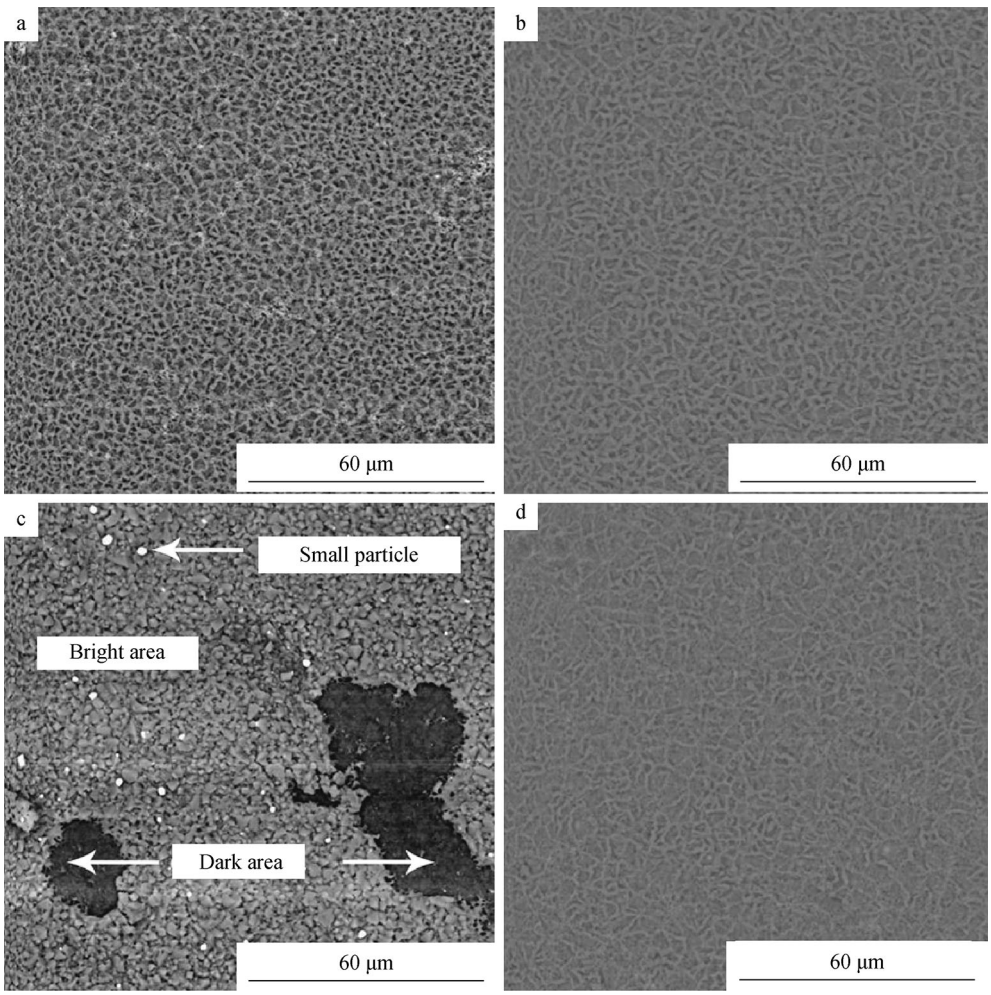

Fig. 3 Surface backscatter images of specimens after 1100 °C/300-h oxidation test **a** 1-μm Pt with 1000 °C/1-h diffusion, **b** 3-μm Pt with 1000 °C/1-h diffusion, **c** 5-μm Pt with 1000 °C/1-h diffusion, **d** 5-μm Pt with 1100 °C/1-h diffusion

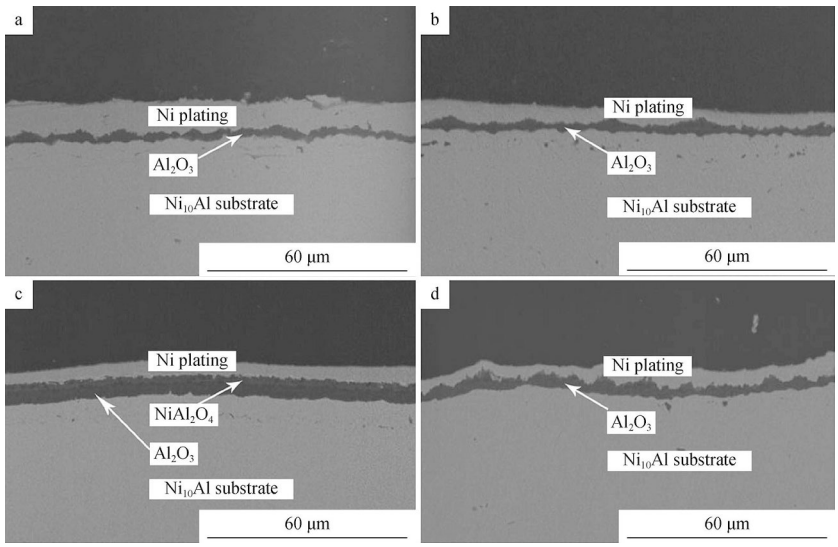

Fig. 4 Cross-sectional backscatter images of specimens after 1100 °C/300-h oxidation test **a** 1-μm Pt with 1000 °C/1-h diffusion, **b** 3-μm Pt with 1000 °C/1-h diffusion, **c** 5-μm Pt with 1000 °C/1-h diffusion, **d** 5-μm Pt with 1100 °C/1-h diffusion

Table 4 Surface elements concentration of Pt-diffused coatings after 1100 °C/300-h oxidation (at%)

No.	Area	Al	Ni	Pt	O
1	Surface	71.98	10.73	–	Bal.
2	Surface	74.27	7.01	–	Bal.
3	Small particles	–	22.67	77.33	–
	Bright area	58.55	26.24	–	Bal.
	Dark area	71.47	5.39	–	Bal.
4	Surface	72.75	8.49	–	Bal.

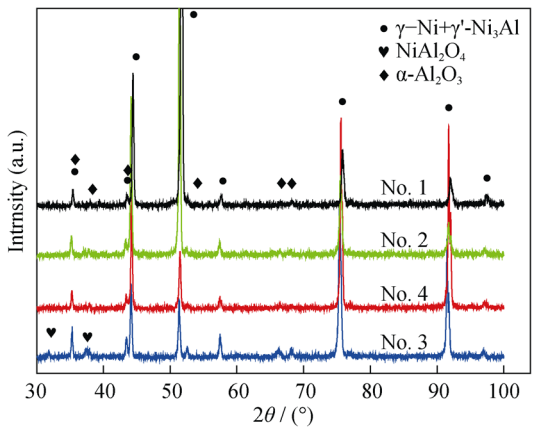

Fig. 5 XRD patterns of specimens after 1100 °C/300-h oxidation test

In the present study, with the same vacuum diffusion process, increasing Pt thickness has a negative effect in high-temperature oxidation, which could be attributed to the defects introduced by electroplating. During low-temperature vacuum diffusion process (1000 °C), inward diffusion flux of Pt is higher than outward diffusion of Ni and Al from substrate, so these defects and cracks are generated near the surface, which could be the short path for oxygen and accelerate the oxidation. As shown in Fig. 6b–d, the surface morphologies of Pt-diffused coatings become coarser with Pt thickness increasing. The cross-sectional back-scattered morphologies of Pt-diffused coatings are shown in Fig. 7, which are typical dark γ-Ni and bright γ′-Ni_3Al phase.

In summary, 1-μm Pt film is sufficient to act as the third element for Al selective oxidation, and increasing Pt thickness does not show any advantage in oxidation resistance with low-temperature diffusion process.

3.3 Effect of diffusion temperature

In order to examine the effect of diffusion temperature, No. 3 and 4 specimens with the same initial Pt thickness (5 μm) were comparatively studied at different diffusion temperatures. As shown in Fig. 2, No. 4 specimen diffused at 1100 °C shows better oxidation resistance than No. 3. In Fig. 6d and e, the surface of No. 4 specimen is smoother than that of No. 3, which has less cracks and defects due to the high diffusion temperature. In summary, thick Pt film needs high-temperature diffusion process, which could diminish the defects in Pt electroplating and make a smoother coating surface.

In the present work, 1-μm Pt-diffused coating has the lowest Al and Pt content in all four coatings and it also has

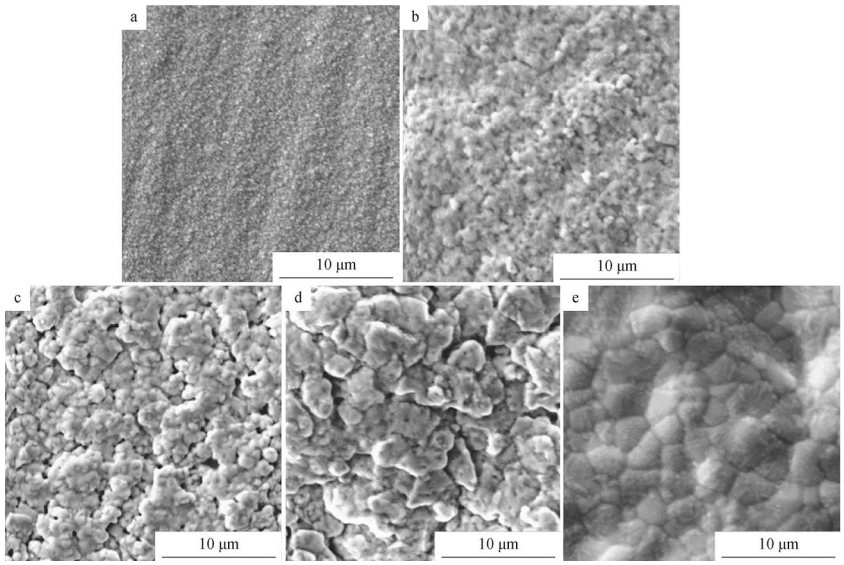

Fig. 6 Surface secondary electron images of specimens **a** 1-μm Pt film, **b** 1-μm Pt with 1000 °C/1-h diffusion, **c** 3-μm Pt with 1000 °C/1-h diffusion, **d** 5-μm Pt with 1000 °C/1-h diffusion, **e** 5-μm Pt with 1100 °C/1-h diffusion

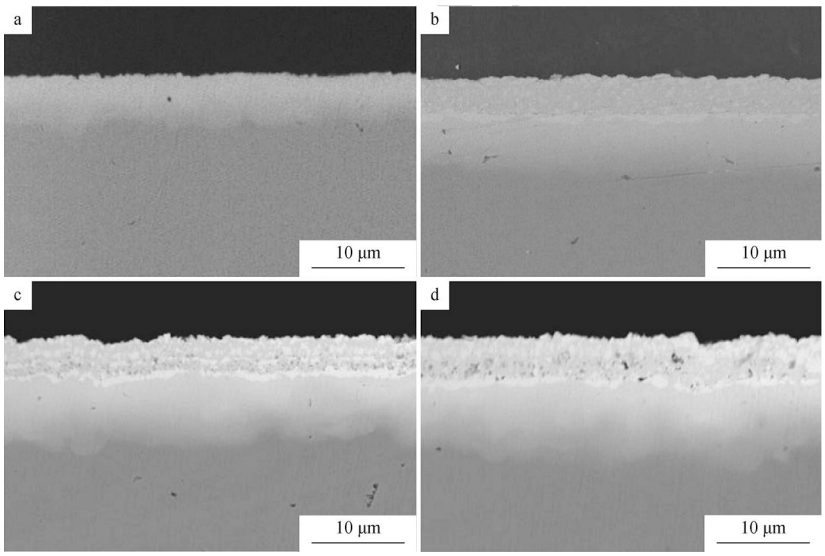

Fig. 7 Cross-sectional back scatter images **a** 1-μm Pt with 1000 °C/1-h diffusion, **b** 3-μm Pt with 1000 °C/1-h diffusion, **c** 5-μm Pt with 1000 °C/1-h diffusion, **d** 5-μm Pt with 1100 °C/1-h diffusion

the finest gain size. As shown in Fig. 6, high-temperature diffusion treatment leads to the growth of grain. The grain size of 1-μm Pt-diffused coating on Ni10Al grows to ~ 267 nm after 1-h diffusion treatment at 1000 °C, whereas 5-μm Pt-diffused coating grows to 1–5 μm after 1-h diffusion treatment at 1100 °C. Grain boundary is a short path for Al and oxygen diffusion. If the grain size is nano-sized, external Al_2O_3 scale could form on NiCrAl alloy even at low Al content [31]. Consequently, 1-μm Pt-diffused coating with nano-sized grain reveals the best oxidation resistance.

4 Conclusion

Pt-diffused coatings were produced by electroplating 1–5-μm Pt films on Ni10Al alloy and then followed by vacuum diffusion treatment at 1000–1100 °C. Pt film reveals nano-sized grain of 93–113 nm, which diffused at 1000 °C keeps nano-sized structure. 1-μm Pt-diffused coating shows the best oxidation resistance even at such low Al (10 at%) and Pt (6 at%) content. Increasing initial Pt thickness would introduce more defects and cracks during vacuum diffusion

process, leading to a duplex scale and decreasing the coating oxidation resistance.

Acknowledgements This research was financially supported by the Nature Science Foundations of China (Nos. 51590894, 51425102 and 51231001).

References

[1] Felten EJ, Pettit FS. Development, growth, and adhesion of Al_2O_3 on platinum–aluminum alloys. Oxid Met. 1976;10(3):189.

[2] Fountain JG, Golightly FA, Stott FH, Wood GC. The influence of platinum on the maintenance of α-Al_2O_3 as a protective scale. Oxid Met. 1976;10(5):341.

[3] Streiff R, Cerclier O, Boone DH. Structure and hot corrosion behavior of platinum-modified aluminide coatings. Surf Coat Technol. 1987;32(4):111.

[4] Tawancy HM, Abbas NM, Rhys-Jones TN. Role of platinum in aluminide coatings. Surf Coat Technol. 1991;49(1):1.

[5] Bouhanek K, Adesanya OA, Stott FH, Skeldon P, Lees DG, Wood GC. Isothermal and thermal cyclic oxidation behaviour of thermal barrier coatings: Pt aluminide bond coats. Mater High Temp. 2000;17(2):185.

[6] Chen MW, Glynn ML, Ott RT, Hufnagel TC, Hemker KJ. Characterization and modeling of a martensitic transformation in a platinum modified diffusion aluminide bond coat for thermal barrier coatings. Acta Mater. 2003;51(14):4279.

[7] Walston WS, Schaeffer JC, Murphy WH. A new type of microstructural instability in superalloys—SRZ. In: Kissinger RD, Deye DJ, Anton DL, Cetel AD, Nathal MV, Pollock TM, Woodford DA, editors. Superalloys. Warrendale: The Minerals, Metals and Materials Society; 1996. 9.

[8] Matsuoka Y, Aoki Y, Matsumoto K, Satou A, Suzuki T, Chikugo K. The formation of SRZ on a fourth generation single crystal superalloy applied with aluminide coating. In: Green KA, Pollock TM, Harada H, Howson TE, Reed RC, Schirra JJ, Walston S, editors. Superalloys. Warrendale: The Minerals, Metals and Materials Society; 2004. 637.

[9] Lavigne O, Ramusat C, Drawin S, Caron P, Boivin D, Pouchou JL. Relationships between microstructural instabilities and mechanical behavior in new generation nickel-based single crystal superalloys. In: Green KA, Pollock TM, Harada H, Howson TE, Reed RC, Schirra JJ, Walston S, editors. Superalloys. Warrendale: The Minerals, Metals and Materials Society; 2004. 667.

[10] Das DK, Murphy KS, Ma SW, Pollock TM. Formation of secondary reaction zones in diffusion aluminide-coated Ni-base single-crystal superalloys containing ruthenium. Metall Mater Trans A. 2008;39(7):1647.

[11] Suzuki A, Rae CMF, Yoshida M, Matsubara Y, Murakami H. Secondary reaction zones in coated 4th generation Ni-based blade alloys. In: Reed RC, Green KA, Caron P, Gabb TP, Fahrmann MG, Huron ES, Woodard SA, editors. Superalloys. Warrendale: The Minerals, Metals and Materials Society; 2008. 777.

[12] Pollock TM, Das DK, Gleeson B, Murphy KS, Ma S. Formation of secondary reaction zone in ruthenium bearing nickel based single crystal superalloys with diffusion aluminide coatings. Mater Sci Technol. 2009;25(2):300.

[13] Adesanya OA, Bouhanek K, Stott FH, Skeldon P, Lees DG, Wood GC. Cyclic oxidation of two bond coats in thermal barrier coating systems on CMSX-4 substrates. In: High Temperature Corrosion and Protection of Materials 5, Pts 1 and 2. Mater Sci Forum. Zürich: Trans Tech Publications Ltd; 2001. 639.

[14] Bouhanek K, Adesanya OA, Stott FH, Skeldon P, Lees DG, Wood GC. High temperature oxidation of thermal barrier coating systems on RR3000 substrates: Pt aluminide bond coats. In: High Temperature Corrosion and Protection of Materials 5, Pts 1 and 2. Mater Sci Forum. Zürich: Trans Tech Publications Ltd; 2001. 615.

[15] Zhang Y, Pint BA, Haynes JA, Wright IG. A platinum-enriched $\gamma + \gamma'$ two-phase bond coat on Ni-based superalloys. Surf Coat Technol. 2005;200(5):1259.

[16] Haynes JA, Pint BA, Zhang Y, Wright IG. Comparison of the cyclic oxidation behavior of β-NiAl, β-NiPtAl and $\gamma + \gamma'$ NiPtAl coatings on various superalloys. Surf Coat Technol. 2007;202(4):730.

[17] Jiang C, Gleeson B. Surface segregation of Pt in γ'-Ni_3Al: a first-principles study. Acta Mater. 2007;55(5):1641.

[18] Haynes JA, Pint BA, Zhang Y, Wright IG. The effect of Pt content on $\gamma + \gamma'$ NiPtAl coatings. Surf Coat Technol. 2008;203(5):413.

[19] Pint BA, Haynes JA, More KL, Schneibel JH, Zhang Y, Wright IG. The performance of Pt-modified alumina-forming coatings and model alloys. In: Reed RC, Green KA, Caron P, Gabb TP, Fahrmann MG, Huron ES, Woodard SA, editors. Superalloys. Warrendale: The Minerals, Metals and Materials Society; 2008. 641.

[20] Wu RT, Kawagishi K, Harada H, Reed RC. The retention of thermal barrier coating systems on single-crystal superalloys: effects of substrate composition. Acta Mater. 2008;56(14):3622.

[21] Zhao X, Xiao P. Effect of platinum on the durability of thermal barrier systems with a $\gamma + \gamma'$ bond coat. Thin Solid Films. 2008;517(2):828.

[22] Mu N, Izumi T, Zhang L, Gleeson B. Compositional factors affecting the oxidation behavior of Pt-Modified γ-Ni + γ'-Ni_3Al-based alloys and coatings. In: High Temperature Corrosion and Protection of Materials 7, Pts 1 and 2. Mater Sci Forum. Zürich: Trans Tech Publications Ltd; 2008. 239.

[23] Hayashi S, Gleeson B. Early-stage oxidation behavior of Pt-modified γ'-Ni_3Al-based alloys with and without Hf Addition. Oxid Met. 2009;71(1):5.

[24] Vialas N, Monceau D. Substrate effect on the high-temperature oxidation behavior of a Pt-modified aluminide coating. Part I: influence of the initial chemical composition of the coating surface. Oxid Met. 2006;66(3):155.

[25] Hou PY, Izumi T, Gleeson B. Sulfur segregation at Al_2O_3/γ-Ni + γ'-Ni_3Al interfaces: effects of Pt, Cr and Hf additions. Oxid Met. 2009;72(1):109.

[26] Pint BA, Haynes JA, Zhang Y. Effect of superalloy substrate and bond coating on TBC lifetime. Surf Coat Technol. 2010;205(5):1236.

[27] Wu RT, Wang X, Atkinson A. On the interfacial degradation mechanisms of thermal barrier coating systems: effects of bond coat composition. Acta Mater. 2010;58(17):5578.

[28] Tawancy HM, Al-Hadhrami LM. Influence of titanium in nickel-base superalloys on the performance of thermal barrier coatings utilizing $\gamma + \gamma'$ Platinum bond coats. J Eng Gas Turbine Power. 2011;133(4):042101.

[29] Niu JM, Wang W, Zhu SL, Wang FH. The scaling behavior of sputtered Ni_3Al coatings with and without Pt modification. Corros Sci. 2012;58(5):115.

[30] Gleeson B, Mu N, Hayashi S. Compositional factors affecting the establishment and maintenance of Al_2O_3 scales on Ni–Al–Pt systems. J Mater Sci. 2009;44(7):1704.

[31] Chen GF, Lou HY. Predicting the oxide formation of Ni–Cr–Al alloys with nano-sized grain. Mater Lett. 2000;45(5):286.